Optik 136 (2017) 564–572

Contents lists available at ScienceDirect

Optik

journal homepage: www.elsevier.de/ijleo

Original research article

Multilayer AR coatings of TiO_2/MgF_2 for application in optoelectronic devices

Waqar A.A. Syed [a,*], Nouman Rafiq [a], Asad Ali [a,b], Rafi-ud Din [c], Wiqar H. Shah [a]

[a] Department of Physics, International Islamic University, Islamabad, Pakistan
[b] Ripha International University, Islamabad, Pakistan
[c] PINSTECH, Islamabad, Pakistan

ARTICLE INFO

Article history:
Received 8 December 2016
Received in revised form 21 February 2017
Accepted 21 February 2017

Keywords:
Multilayer coatings
TiO_2
MgF_2
Anti-reflection coatings

ABSTRACT

A multilayer system of 10 alternating TiO_2 and MgF_2 thin film was prepared on BK7 glass substrate by electron beam and resistive thermal evaporation techniques respectively. The substrate with 20 mm diameter and thickness of 1 mm were placed in a vacuum chamber at partial pressures of 10–5 mbar for TiO2 and 10–6 mbar for MgF2 film respectively. The as-deposited films were annealed at 400 °C for an hour in ambient environment. The structural, optical and morphological properties were studied by XRD, UV–vis spectrophotometer, ellipsometery and scanning electron microscopy (SEM) respectively. The structural analysis confirms that all the thin films samples were polycrystalline in nature with tetragonal and rhombohedra phases. SEM analysis confirms the uniformity of surface and quite stable multilayer thin film structure without any micro cracks. Ellipsometery studies were carried out and refractive index and extinction coefficient as function of wavelength are obtained. The samples are found highly transparent in the range of 400–800 nm, whereas the overall absorption and reflection of the multilayer thin film was decreased for the annealed samples. It has been demonstrated that the residual reflectance of the AR coating can be significantly reduced by combining the multilayer systems with an outermost low index layer made of MgF_2. The realization of such hybrid multilayer systems are extremely useful as front surface of the photovoltaic cells, optoelectronic devices and front mirror for laser.

1. Introduction

Antireflection coatings have been in use since long to overcome the problem due to Fresnel's reflections, which significantly reduces intensity of transmitted light [1]. It is now established that the application of multilayer coating on the front surface of the photovoltaic cells or optoelectronic devices reduces the reflection of the incident light improving the device performance [2,3]. These coatings are widely used in solar cells, lenses, optical window for lasers and display windows etc [4]. Bruynooghe et al. [5] described the nature as an example of so-called 'moth-eye structures', preventing reflections by gradually changing refractive index from the air to substrate. A graded transition between the refractive indices of two interfacing media has perfect 'anti-reflection' properties. Typically the AR coating is fabricated by using a single layer coating of a material, or a doubled layer of two selected materials. There are limited but important applications which may involve larger number of layers for example if a wide band of wavelengths is needed to be covered.

* Corresponding author.
E-mail address: adil.syed@iiu.edu.pk (W.A.A. Syed).

http://dx.doi.org/10.1016/j.ijleo.2017.02.085
0030-4026/

Several techniques are used for multilayer deposition; sol–gel processing is one of them which has widely been applied for the preparation of thin films either of inorganic or hybrid polymer compositions [6]. A wet chemical route is an efficient method for making k/4 antireflective films [7,8]. However sol-gel technique is found not very advantageous for making a bit dense materials and therefore physical vapor deposition (PVD) or chemical vapor deposition (CVD) techniques are preferred.

Schuler et al. [9] have reported fabrication of denser columnar microstructure for Al-doped zinc-oxide thin film and similar work on titania thin films was reported by Wang et al. [10]. Recently Bittener et al. [11] have demonstrated the dense TiO_2 combined with low-refractive porous MgF_2 coatings for the preparation of optical interference assemblies. Hegmann et al. [12] have described that how the microstructure of the respective films can be affected by multiple coating techniques. The single layer metal coatings usually provide high reflection power over wide range of wavelengths, however at the cost of the absorbance and transmission, which are very small. The broadband multiple layer coatings may provide the ability to design with very low reflectance with much better performance as compared to single layer coatings. When compared at specific wavelengths, a broadband multilayer coating can perform ten times better than a broadband single layer coating.

MgF_2 is the one of lowest refractive index material i.e. 1.38, used for antireflection coatings. Due to its low refractive index, substrate materials with higher refractive indices such as TiO_2 [13], Sc_2O_3 [14], CeO_2 [15], Al_2O_3 [16,17] and LaF_3 [18–21] are used in optical multilayer structures. These multilayers have been used for a variety of optical applications. Single layer anti-reflective coating of MgF_2 might exhibit reflectivity of about 2% at 550 nm, which is about an order of magnitude greater than the reflectivity of multilayer coatings for same wavelength. MgF_2 film contains crystallites in its structure; their grain boundaries cause an absorption tail for the refractive index below the material's band gap. Thin films of TiO_2 with high reflectivity over wide range of spectrum, is suitable for dielectric multilayer mirrors. Keeping in view the optimization carried out in the reference [22], TiO_2 was selected as the high reflective index materials.

Narrow band multilayer coatings have outperformed the broadband coatings for specific wavelengths; commonly called V-coats, as the performance plot looks like the letter "V". Antireflection from a multilayer structure requires a transitive material layer sandwiched between two reflective material layers. Therefore a multilayer structure is composed of a combination of material with alternating high and low refractive indices and alternate reflections at more than one boundaries [23]. Exact knowledge about optical properties of MgF_2 thin film can help producing AR or HR thin films of required parameters for the possible use as front mirror of lasers [15,24].

One of the major problems with thin films of dielectric materials fabricated by physical vapor deposition (PVD) is the porosity, which usually form columnar porosities with various diameters. The residual air or water in these porosities can affect optical and other properties. Therefore, a significantly higher temperature is provided to the substrate temperature during the PVD process. Ar^+ lasers are commercially available with various powers operating on both blue (476.5 nm, 488 nm) and green (514.5 nm) transitions simultaneously. One of the purpose of this study is to investigate the MgF_2 and TiO_2 multilayer coatings as front window of the photovoltaic cells and optoelectronic devices in particular with anti-reflecting for blue and green wavelength argon ion lasers.

2. Experimental work

In the present work, 99.99% pure MgF_2 and TiO_2 in powder form were obtained from Sigma Aldrich and used as source materials for the preparation of multilayer of TiO_2 and MgF_2 thin films. The substrate was BK7 glass slides with a thickness of 1 mm and diameter 20 mm. These multilayer thin films were deposited by vacuum electron beam evaporation and thermal evaporation techniques respectively.

For proper adhesion of the films, the glass substrates were first cleaned with acetone, and dip into the ultrasonic cleaner having distilled water, mixed with chemical agent for twenty minutes. The substrate was than washed with fresh water and finally dried up with nitrogen gas gun. The target materials were placed in the vacuum coating plant. The rotary and diffusion pumps were used to evacuate the vacuum chamber up to 10^{-6} mbar. The substrates were pre-heated up to 250 °C, which was in order to remove the contamination. Substrate holders were kept rotating for about 20 rev/min, for the uniformity of thin film. The system was set for the evaporation of MgF_2 at the rate of 0.75 nm/s with help of thermal sources at 10^{-6} mbar pressure, while TiO_2 was evaporated with the rate of 0.50 nm/s by electron beam evaporation sources at pressure 10^{-5} mbar to obtain TiO_2/MgF_2 multilayer thin films.

These samples of different thickness were prepared on substrate, already polished with backside to avoid any reflections. The deposition parameters for all three samples are summarized in Table 1. All synthesized samples were annealed at 400 °C for one hour. The structural, morphological and optical characterizations were carried out by X-ray diffraction (XRD), scanning electron microscope (SEM), UV–vis spectrometer and Ellipsometry.

3. Results and discussion

3.1. Structural properties

The structural properties of fabricated thin films were studies by XRD and phase structure and the crystallinity parameters were determined. The diffraction pattern of thin films was recorded on Philip Diffractmeter instrument using Cu-Kα radiations of wavelength 1.54 Å. The diffraction patterns for all three samples are shown in Figs. 1–3, relieving polycrystalline structure of samples. The peak positions confirm the crystallographic nature of TiO_2 and MgF_2 films as tetragonal

Table 1
Deposition parameters of sample A,B and C, with substrate temperature of 250 °C.

Sample with No. of layers	Target Material	Voltage (KV)	Chamber Pressure (mbar)	Deposition rate (nm/sec)	Film thickness (nm)	% Transmittance
Sample-A with 10 layers	TiO_2 For layers 1,3,5,7,9	7.5	7.3×10^{-5}	0.18	46.12	99.36
	MgF_2 For layers 2,4,6,8,10	4	10^{-6}	0.75	252.8	
Sample-B with 10 layers	TiO_2 For layers 1,3,5,7,9	7.5	7.3×10^{-5}	0.18	39.81	99.32
	MgF_2 For layers 2,4,6,8,10	4	10^{-6}	0.75	218.26	
Sample-C with 10 layers	TiO_2 For layers 1,3,5,7,9	6.5	7.0×10^{-5}	0.18	90.26	99.07
	MgF_2 For layers 2,4,6,8,10	4	2.0×10^{-6}	0.75	150.43	

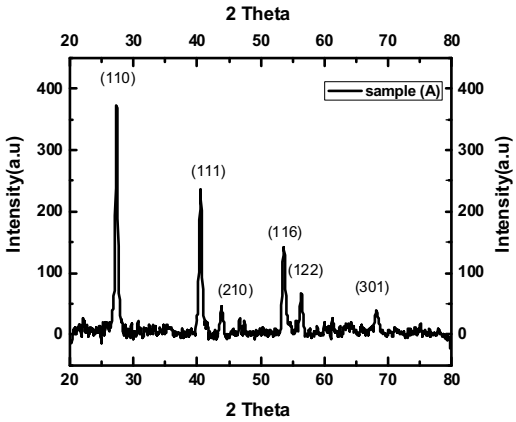

Fig. 1. Diffraction pattern of sample A.

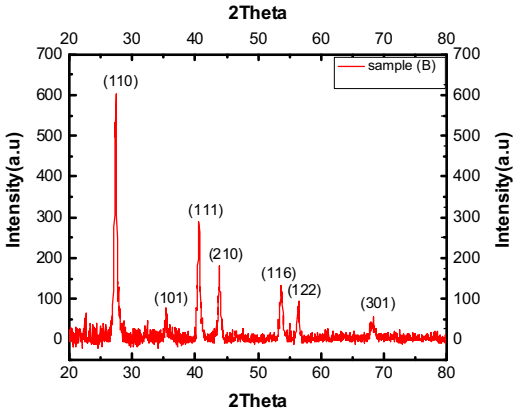

Fig. 2. Diffraction pattern of sample B.

shapes, similar to the rutile structure of the bulk TiO_2 and MgF_2. It seems that electron beam evaporation techniques, as well as substrates heating, enhances the crystalline phase of the TiO_2 and MgF_2 film respectively. These results are in good agreement with Atanassovet al. [25]. as the crystallization of MgF_2 thin films starts forming at temperatures above 250 °C.

The obtained peaks were matched with JCPDS cards No. (00-041-1443, 00-010-0063). Most of the peaks match with MgF_2 while a few peaks related to TiO_2 are also identified. The planes (110), (101), (111), (210) and (301) of MgF_2 with tetragonal structure and (116) and (122) planes of TiO_2 with rhombohedra structure were confirmed.

Fig. 4 shows the crystallite size determined by the Scherrer-formula of the MgF_2 and TiO_2 single and multilayer on BK7 glass independent of the single layer thickness. The single layer thicknesses of the multilayer assemblies were calculated

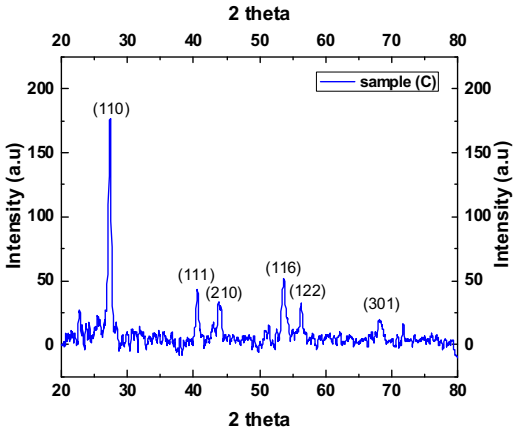

Fig. 3. Diffraction pattern of sample C.

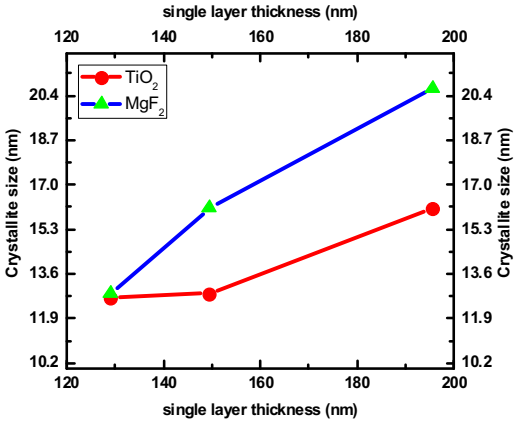

Fig. 4. MgF_2 (triangle) and TiO_2 (square) crystallite size as function of single layer thickness.

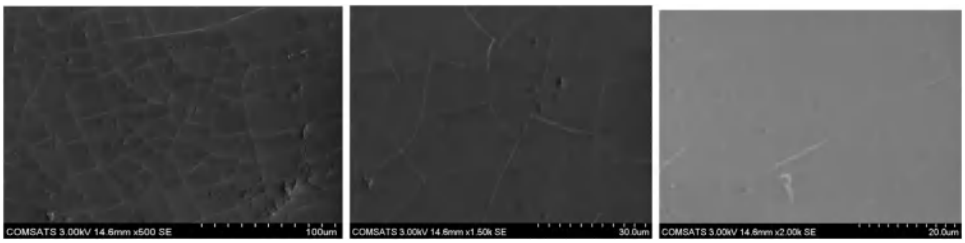

Fig. 5. SEM images of sample A.

dividing the total thickness through the number of coatings. The results show that the decreasing thickness of MgF_2, effect respective increase in crystallite growth. The calculated crystallite size of the MgF_2 single layer is larger than TiO_2.

3.2. Surface properties

The surface morphology was examined with the help of SEM; images are given in Figs. 5–7. Both the multilayer assemblies exhibit non-porous, homogeneous and denser microstructure. Although the SEM investigation gives a first qualitative glance at the film morphology, no detailed information regarding porosity and average pore size can be obtained. The surface morphology of the films was denser and more uniform compared with the as-deposited film. These results indicated that an extremely flat and uniform multilayer film was obtained by using electron beam and resistive thermal evaporation techniques, which was suitable for application in optical films. Due to compressive TiO_2 films and small tensile stress of MgF_2, multilayer thin film is quite stable without any micro cracks.

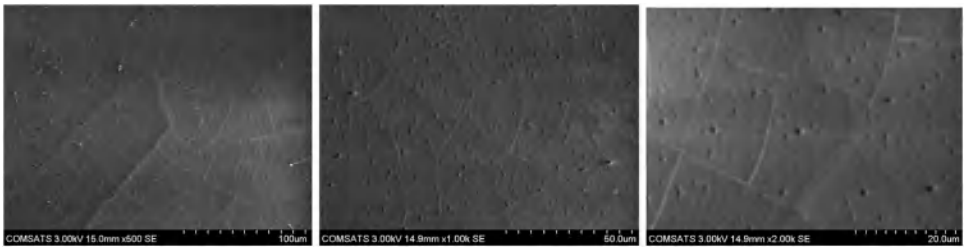

Fig. 6. SEM Images of sample B.

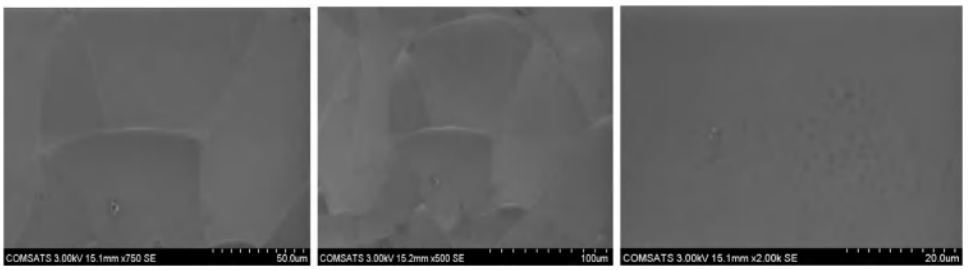

Fig. 7. SEM images of sample C.

3.3. Optical properties

The quality of anti-reflection (AR) coating can be improved by increasing transmission, enhancing contrast, and eliminating ghost images. Most AR coatings are durable with high resistance to physical or environmental damage and significantly improve the performance of an optical system. The coating is designed so that the relative phase shift between the beam reflected at the upper and lower boundary of the thin film is 180°. Destructive interference between the two reflected beams occurs, cancelling both beams before they exit the surface. The optical thickness of the coating must be an odd number of quarter wavelengths λ/4, where λ is the design wavelength.

3.3.1. Transmission

The transmission properties of a coating depend on the wavelength of light being used, the refractive indices of substrate and coating, the thickness of the coating, and the angle of the incident light. The optical transmission spectra of as-deposited and annealed samples at 400 °C were recorded as a function of wavelength in the range 400–800 nm, shown in Fig. 8. The transmission spectrum shows that the samples were highly transparent in visible region particularly in range of 450–650 nm. After annealing a little decline in transmission and whole spectrum is shifted towards lower wavelengths. One of the important purpose of this study is to investigate the MgF_2 and TiO_2 multilayer coatings as an anti-reflecting for argon ion laser. These lasers are commercially available in both blue (476.5 nm, 488 nm) and green (514.5 nm) transitions simultaneously. The multilayer samples are highly transparent for argon laser wavelengths and very suitable as anti-reflective front mirror.

The optical matrix approach is a method which is based on matching the electric and magnetic field strengths of the incident light on the interface of multilayer. For N-layer antireflection coating, the matrix relation is defined as [26],

$$R = \left[\frac{n_0 - Y}{n_0 + Y}\right]\left[\frac{n_0 - Y}{n_0 + Y}\right]^{*} \tag{1}$$

Where Y is optical admittance, which is the ratio of electric and magnetic field amplitude and n_0 is refractive index of air. Each layer of coating may be defined by a matrix of the from,

$$M_j = \begin{bmatrix} cos\delta_j & isin\delta_j \\ in_j sin\delta_j & cos\delta_j \end{bmatrix} \tag{2}$$

where $n_p = y_j/cos\theta$, $n_s = y_j cos\theta$ are for p and s polarizations respectively. $\delta_j = \left[2\pi\left(n_j \#XPS\#ndash; ik_j\right) d_j cos\theta_j\right]/\lambda$, $n_0 sin\theta_0 = n_j \sin\theta_j$ and δ_j, y_j, n_j, d_j, θ_j and λ are the phase shift, optical admittance, refractive index, thickness, incident angle and wavelength respectively. Duyar et al. simulated the transmittance curve for 8 layers of AR coatings and obtained more than 99% transmittance, which is 10% higher than that of uncoated glass. Our results are in good agreement with above simulation [26].

Fig. 9 shows the optical transmission for all samples after annealing; all samples are highly transparent (above 99%) in 450–650 nm and summary is presented in Table 1. In sample A, percentage transmittance is highest (99.36) and covers the maximum range of wavelength 450–660 nm, whereas for sample B the spectra is shifted towards lower wavelengths and

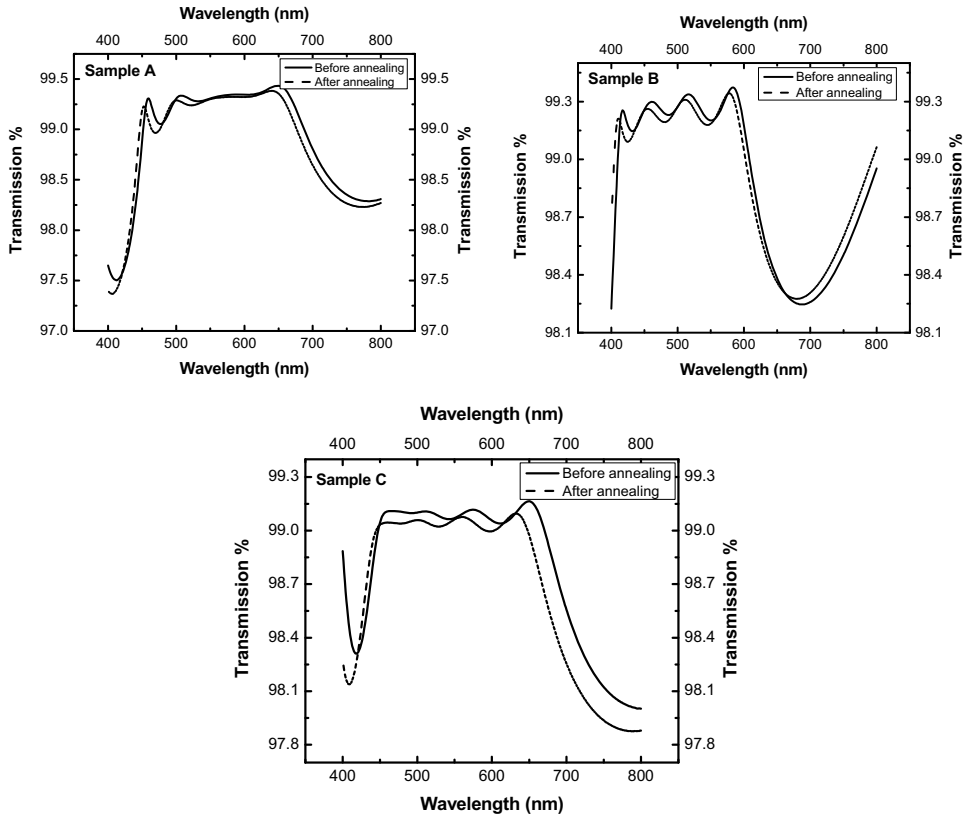

Fig. 8. Transmission spectra of TiO_2 and MgF_2 multilayer thin film before and after annealing.

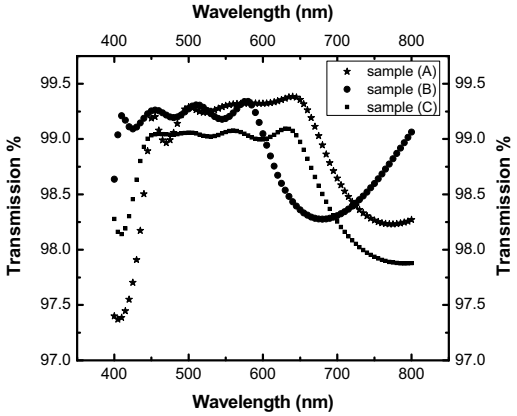

Fig. 9. Combined transmission spectra for all samples.

shows a deviation from 450 to 410 nm and the%transmission is reduced to 99.32%. The lowest transmission is found for sample C has (99.07%) as compare to other samples.

3.3.2. Reflection

The reflection coefficient depends upon radiation energy as well as composition of film. In Fig. 10 shows reflection spectra of TiO_2 and MgF_2 multilayer thin film of sample A, sample B and sample C and also a comparison of annealed samples is shown in (d). Interference minima and maxima due to multiple reflections on film surfaces can be observed, showing that the films have a homogenize surface. The reflection is extremely low for all the samples showing high transparent samples in visible region and suitable for argon laser. In Table 2, a comparison of present work with similar kind of previous work is given; a significant improvement more than an order of magnitude is evident.

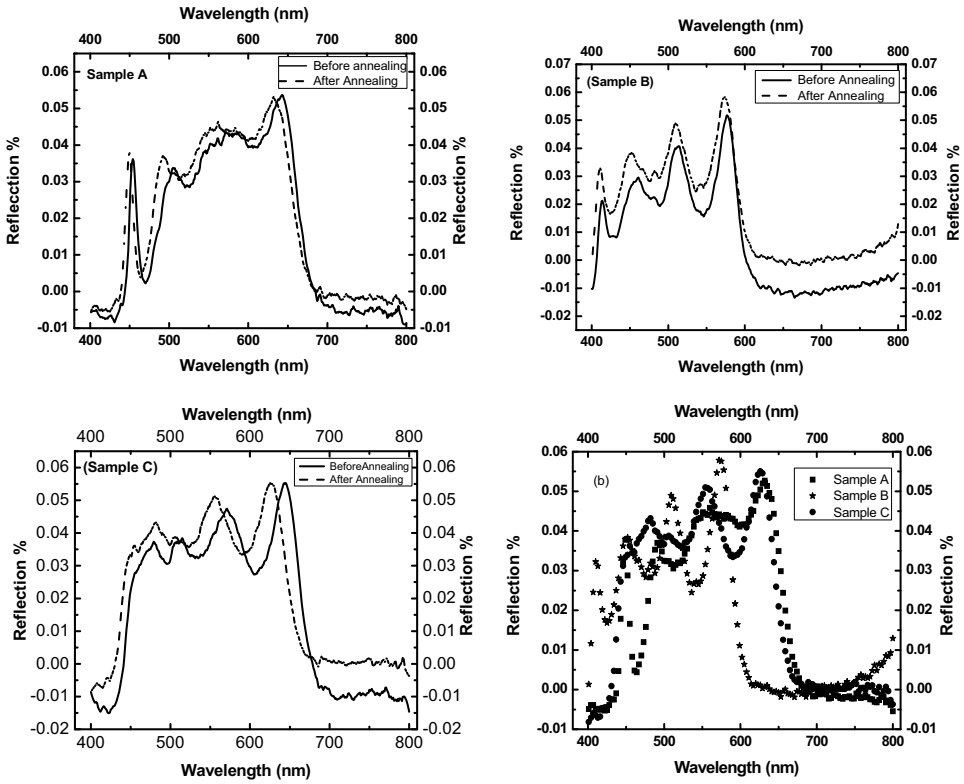

Fig. 10. **(a)** Reflection spectra of TiO_2 and MgF_2 thin film of samples A, B and C. **(b)** Reflection spectra of all annealed samples.

Table 2
Comparison of antireflection coating of different materials.

Sr. No.	Reflection%	Range(nm)	Materials	Layers	Substrate	References
1	0.04	450–650	TiO_2/MgF_2	10	Bk7	Our results
2	1.7	400–1700	Nb_2O_5, SiO_2	14	Bk7	[4]
3	0.5	400–1700	MgF_2, SiO_2	8	Bk7	[4]
4	3.3	400–800	Al_2O_3/TiO_2	2	Silicon	[28]
5	6.2	400–1000	SiO_2/TiO_2	2	Silicon	[29]
6	3.2	400–1000	SiO_2/TiO_2- SiO_2/TiO_2	3	Silicon	[31]
7	3	800–1100	$MgF_2/Al_2O_3/ZnS$	3	Silicon	[30]
8	3	450–650	ZnS-MgF_2	1	GaAs	[31]
9	4	500–1000	ZnS-MgF_2	2	GaAs	[33]
10	5	550–1200	ZnS-MgF_2	3	GaAs	[33]

3.4. Ellipsometry measurements

In optical coatings, there are two types of graded index profiles i.e. precisely controlled inhomogeneous graded optical coatings and homogeneities arise from the instability of the deposition process [27]. The second one is caused by micro structural changes, impurities or the interaction of source material with the substrate. One can consider the reflectance for both transparent and absorbing substrates and obtain expressions for the minima and maxima of the transmittance or reflectance curves. The refractive index is usually higher with these assumptions that extinction coefficient is much smaller than the value of refractive index. Once a material is deposited, its refractive index will not be altered by any successive and more importantly the substrate is considered semi-infinite, which means that the contribution to the reflectance from the back side is negligible.

The multilayers were examined using a spectroscopic ellipsometer (Sentech SE850). Ellipsometry is used to measures the change of polarization of light upon reflection from the sample surface. The normal task of an ellipsometer is to determine layer thickness and optical properties of single or multilayer surfaces. The data were collected in the 300–900 nm spectral range. Incident angles were chosen near the Brewster angle to minimize the effect of systematic errors and random noise on the measured data. One side polished glass substrates were employed to avoid any unwanted reflections from the backside.

The refractive index as a function of visible wavelengths of all samples is plotted in Fig. 11; the refractive index decreases rapidly from 325 to 600 nm and become linear after 600–800 nm. The refractive index varies in the range from 1.36 to

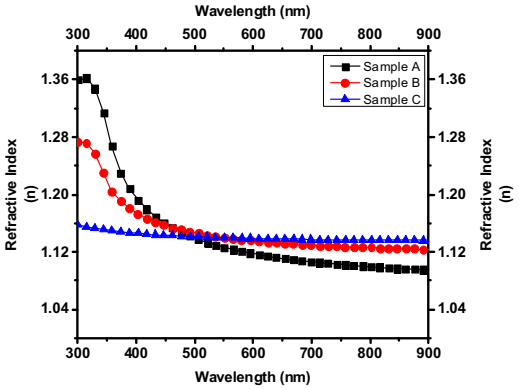

Fig. 11. Comparison of Refractive index of all samples as a function of wavelength.

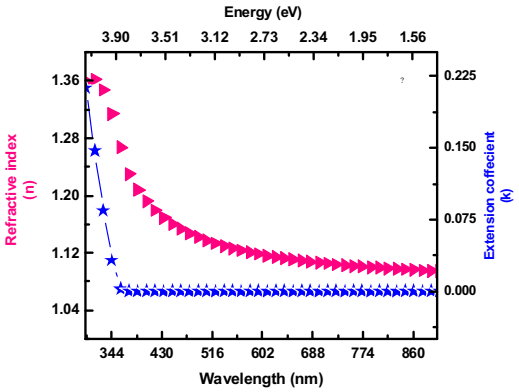

Fig. 12. Refractive index (stars) and extension coefficient (triangles) as a function of wavelength for sample A.

1.09. The correlation of single layer thickness and total thickness of the multilayer assemblies was considered to be linear. Overall thicknesses of sample 1, 2 and 3 are 1494.6, 1290.35, 1203.45 nm respectively. The sample 1 of 10-fold layer is much denser and homogenous microstructure. For the TiO_2 layers, the effect of a columnar growth was observed in [18]. To further investigate this and the densification of the multilayer, a significant densification and decrease of the refractive index can be measured, only if the single layer thickness is increased. The 10-fold layer has the refractive index less than to that of crystalline MgF_2 ($n = 1.38$), for sample A and reduces sharply after 350 nm and becomes linear at 450 nm, approximately 1.09. However for sample C, the calculated refractive index of the backbone material is even so small to that of crystalline MgF_2 as shown in Fig. 12 where refractive index and extension coefficient are plotted as function of wavelength for sample A. These findings correspond very well with already known information from on TiO_2 [30], however dense crystalline MgF_2 coatings by resistive thermal evaporation growth can be detected. This implies that there are no reactions between the two materials or the two materials and the substrate.

4. Conclusion

Structural, optical and surface analysis of the as deposited and annealed multilayer of TiO_2 and MgF_2 prepared by electron beam evaporation and resistive thermal evaporation techniques respectively was investigated. Structural analysis confirms that all the thin films are polycrystalline in nature. Substrate baking of TiO_2 films results in a densely-packed microstructure, due to the thermal energy and momentum transferred from the electron-beam which further causing decrease in extinction coefficient and roughness of the surface. The optical properties have been examined by ellipsometry and a low-index character and the effective refractive index profile has been determined.

The MgF_2 films at substrate temperature of 250 °C results in a maximum transmittance in the visible region. We found that the multilayer thin film structure has quite stable without any micro cracks, due to compressive TiO_2 films and small tensile stress of MgF_2 films. Due to thermal evaporation and electron beam evaporation techniques, TiO_2 and MgF_2 multilayer can be fabricated for many optical coatings, i.e. high-efficiency polarization beam splitters, broadband high reflectors, broadband antireflection coatings and narrow band-pass filters etc. The overall absorption and reflection of the multilayer thin film was decreased for the annealed samples. It has been demonstrated that the residual reflectance of the AR coating can be

significantly reduced by combining the multilayer systems with an outermost low index layer made of MgF_2. The realization of such hybrid multilayer systems appears to be a promising and convenient for the use in optoelectronic devices.

Acknowledgement

The authors would like to thanks Dr. NA Shah of COMSATS Institute Islamabad for useful discussion.

References

[1] L. Rayleigh, On reflection of vibrations at the confines of two media between which the transition is gradual, Proc. London Math. Soc. 1 (1) (1879) 51–56.
[2] J. Zhao, M.A. Green, Optimized antireflection coatings for high-efficiency silicon solar cells, IEEE Trans. Electron Devices 38 (8) (1991) 1925–1934.
[3] J.T. Cox, G. Hass, Antireflection coatings for optical and infrared optical materials Physics of Thin Films Collec., 2, Academic Press, New York, 1964.
[4] O. Duyar, H.Z. Duruosoy, Design and preparation of antireflection and reflection optical coatings, Turk. J. Phys. 28 (2003) 139.
[5] S. Bruynooghe, D. Tonova, M. Sundermann, T. Koch, U. Schulz, Antireflection coatings combining interference multilayers and a nanoporous MgF_2 top layer prepared by glancing angle deposition, Surf. Coat. Technol. 267 (2015) 40–44.
[6] G. Schottner, Hybrid sol-gel-derived polymers: applications of multifunctional materials, Chem. Mater. 13 (2001) 3422–3435.
[7] W. Glaubitt, P. Lobmann, Antireflective coatings prepared by sol- gel processing: principles and applications, J. Eur. Ceram. Soc. 32 (2012) 2995–2999.
[8] W. Glaubitt, P. Löbmann, Anti-soiling effect of porous SiO_2 coatings prepared by sol-gel processing, J. Sol-Gel Sci. Technol. 59 (2011) 239–244.
[9] T. Schuler, M. Aegerter, Optical, electrical and structural properties of sol gel ZnO: al coatings, Thin Solid Films 351 (1999) 125–131.
[10] C. Wang, J. Meinhardt, P. Lobmann, Growth mechanism of Nb-doped TiO_2 sol-gel multilayer films characterized by SEM and focus/defocus TEM, J. Sol-Gel. Sci. Technol. 53 (2010) 148–153.
[11] A. Bittner, A. Schmitt, R. Jahn, P. Lobmann, Characterization of stacked sol–gel films: comparison of results derived from scanning electron microscopy, UV–vis spectroscopy and ellipsometric porosimetry, Thin Solid Films 520 (2012) 1880–1884.
[12] J. Hegmann, P. Lobmann, Sol–gel preparation of TiO_2 and MgF_2 multilayers, J. Sol. -Gel. Sci. Technol. 67 (2013) 436–441.
[13] Y.J. Lee, J.H. Lee, Y.Y. Lee, Y.H. Kang, Y.S. Kim, S.N. Kwon, K. Jeong, Interdiffusion in vacuum-deposited dielectric thin films, Opt. Commun. 190 (1) (2001) 211–220.
[14] S. Tamura, S. Kimura, Y. Sato, S. Motokoshi, H. Yoshida, K. Yoshida, influence of deposition parameters on laser damage threshold of 355-nm scandium oxide-magnesium fluoride high-reflector coatings, Jpn. J. Appl. Phys. 29 (1990) 1960–1962.
[15] S.E. Lee, S.W. Choi, J. Yi, Double-layer anti-reflection coating using MgF_2 and CeO_2 films on a crystalline silicon substrate, Thin Solid Films 376 (1) (2000) 208–213.
[16] S. Shuzhen, S. Jianda, L. Chunyan, Y. Kui, F. Zhengxiu, C. Lei, High-reflectance 193 nm Al 2 O 3/MgF 2 mirrors, Appl. Surf. Sci. 249 (2005) 157–161.
[17] M. Zhan, W. Gao, T. Tan, H. He, J. Shao, Z. Fan, Study of Al 2 O 3/MgF 2 HR coatings at 355 nm, Vacuum 79 (1) (2005) 90–93.
[18] S. Guenster, D. Ristau, A. Gatto, N. Kaiser, M. Trovo, F. Sarto, Proceedings of the 26th international free electron conference FEL, in: R. Bakker, L. Giannessi, M. Marsi, R. Walker (Eds.), Comitato ConferenzeElettra, Trieste, Italy, 2004, pp. 233–236.
[19] E. Welsch, K. Ettrich, H. Blaschke, N. Kaiser, Excimer laser interaction with dielectric thin films, Appl. Surf. Sci. 96 (1996) 393–398.
[20] Z. Czigany, M. Adamik, N. Kaiser, 248 nm laser interaction studies on LaF_3/MgF_2 optical coatings by cross-sectional transmission electron microscopy, Thin Solid Films 312 (1998) 176–181.
[21] S. Jakobs, A. Duparré, H. Truckenbrodt, AFM and light scattering measurements of optical thin films for applications in the UV spectral region, Int. J. Mach. Tools Manuf. 38 (1998) 733–739.
[22] G.D. Wilk, R.M. Wallace, J.M. Anthony, High-κ gate dielectrics: current status and materials properties considerations, J. Appl. Phys. 89 (2001) 5243–5275.
[23] M.A. Ordal, J.B. Robert, R.W. Alexander, L.L. Long, M.R. Querry, Optical properties of Au, Ni, and Pb at submillimeter wavelengths, Appl. Opt. 26 (1987) 744–752.
[24] J.C. Tinoco, E. Magali, I. Benjamín, A. Cerdeira, Conduction mechanisms of silicon oxide/titanium oxide MOS stack structures, Microelectron. Reliab. 48 (2008) 370–381.
[25] G. Atanassov, J. Turlo, J.K. Fu, Y.S. Dai, Mechanical optical and structural properties of TiO2 and MgF2, thin films deposited by plasma ion assisted deposition, Thin Solid Films 342 (1999) 83–92.
[26] Ozlem Duyar, Huseyin Zafer Durusoy, Design and preparation of antireflection and reflection optical coatings, Turk J. Phys. 28 (2004) 139–144.
[27] B.G. Bovard, Rugate filter theory: an overview, Appl. Opt. 32 (1993) 5427–5442.
[28] D.S. Wuu, C.C. Lin, C.N. Chen, H.H. Lee, J.J. Huang, Properties of double-layer Al_2O_3/TiO_2 antireflection coatings by liquid phase deposition, Thin Solid Films 584 (2015) 248–252.
[29] S.Y. Lien, D.S. Wuu, W.C. Yeh, J.C. Liu, Tri-layer antireflection coatings (SiO_2/SiO_2–TiO_2/TiO_2) for silicon solar cells using a sol–gel technique, Solar Energy Mater. Solar Cells 90 (2006) 2710–2719.
[30] D. Bouhafs, A. Moussi, A. Chikouche, J.M. Ruiz, Design and simulation of antireflection coating systems for optoelectronic devices: application to silicon solar cells, Sol. Energy Mater. Sol. Cells 52 (1998) 79–93.
[31] S.M. Jung, Y.H. Kim, S.I. Kim, S.I. Yoo, Design and fabrication of multi-layer antireflection coating for III-V solar cell, Curr. Appl. Phys. 11 (2011) 538–541.